Cytometry PART A
Journal of Quantitative Cell Science

Methods for Cell Volume Measurement

Michael A. Model*

Department of Biological Sciences, Kent State University, Kent, Ohio

Received 11 April 2017; Revised 19 May 2017; Accepted 26 May 2017

Grant sponsor: Kent State University Research Council.

*Correspondence to: Michael Model; Department of Biological Sciences, Cunningham Hall, Kent, OH 44242. E-mail: mmodel@kent.edu

Published online 16 June 2017 in Wiley Online Library (wileyonlinelibrary.com)

DOI: 10.1002/cyto.a.23152

• **Abstract**

Volume is an essential characteristic of a cell, and this review describes the main methods of its measurement that have been used in the past several decades. The discussed methods include various implementations of light scattering, estimates based on one or two cell dimensions, surface scanning, fluorescence confocal and transmission slice-by-slice imaging, intracellular volume markers, displacement of extracellular solution, quantitative phase imaging, radioactive methods, and some others. Suitability of these methods to some typical samples and applications is discussed. © 2017 International Society for Advancement of Cytometry

• **Key terms**

cell volume; cell size; methods; measurements; Coulter; confocal; volume exclusion; quantitative phase

Introduction

Measuring the volumes of complex objects has never been simple, as we know from the example of Archimedes. Perhaps his method has never been surpassed in elegance and accuracy, but what works for a golden crown does not work for biological cells. Thus, a wide variety of methods have been developed, ranging from simple observation under a light microscope to optical computer tomography. And yet, the only method that at present can qualify as "standard" is electronic sizing of cell suspensions. Flow cytometric scattering is popular, too, because of the wide availability of flow cytometers. For measuring adherent cells, everyone seems to have their own preferences. Some methods rely on custom-built instruments, others use standard equipment; some report relative changes, others produce absolute numbers; some measure the total cell volume, others are only sensitive to the osmotically active fraction. To navigate through these multiple options, a comprehensive review would be helpful, but so far, there have been few reviews of the measurement methodology (1–7). This work is an attempt to organize and assess various experimental approaches to cell volume measurement that have been used in the last several decades. The focus is on measurements of individual cells, either attached or in suspension, but excluding larger tissues and organs.

The biological relevance of cell volume will be only marginally considered here, as it has been reviewed multiple times (8–10). Suffice to say that the need to know cell volume frequently arises in studies of cell growth and cell death, osmotic behavior, membrane transport, physiology of blood and kidneys, brain edema, cryopreservation, some aspects of metabolisms and microbial ecology. At the time of this writing, a search for "cell volume" on Google Scholar produces well over a million results.

Components of the Cell Volume

Before proceeding to discuss volume measurement methods, it would be useful to review the components of cell volume and the typical types of experiments that require its knowledge. About 15% of the volume of a resting cell (the numbers can

ISAC International Society for Advancement of Cytometry

vary depending on the cell type) is occupied by organic (or "dry") matter—proteins, nucleic acids, lipids, amino acids, and so forth. Accumulation of organic matter is brought about by intake of small molecules and by metabolism.

The rest of the cell consists of water with dissolved inorganic ions. Not all cellular water is the same: part of it is tightly bound to macromolecules and is known as "osmotically inactive." The larger part of intracellular water can freely exchange with the environment across the plasma membrane.

In many situations, one is mostly concerned with the total volume contained within the cell's outer boundary. This would be a natural parameter if one is interested in the rate of cell growth, for example. The total volume is equally useful in studies of membrane water permeability, which is measured by the rate of osmotically driven intake or expulsion of water. Although the real object of interest here is the volume occupied by intracellular water, one assumes that *rapid* volume changes occur almost entirely by water redistribution. Conversely, slower changes in the volume may occur both by changes in water and in organic matter. If one wishes to separate these two types of contributions to the overall change in cell volume, at least two parameters must be determined: they could be, for example, the total volume and cell dry mass or the total volume and the volume fraction occupied by water. Methods of measurements should be chosen appropriately for the task.

Paper Organization

In the review that follows, we start with methods where cell volume is derived from equivalent displacement of liquid by intact cells. The Coulter technique directly generates cell volume data without additional processing. Absorption and fluorescence exclusion imaging use liquid displacement to measure the heights of individual cells; the lateral dimensions are obtained from regular microscopic projections. The last method included in the first group estimates the average height of a confluent cell layer adhered to the inner side of a capillary. The second group of methods measure or estimate cell volumes from one, two or three dimensions of single cells; it includes the popular confocal microscopy as well as several other techniques. Quantitative phase microscopy and tomography make a third group, where cell volume is measured more or less directly using a more specialized instrumentation. Next, we turn to methods that quantify relative changes in the volume (specifically, those of intracellular solvent water) from concentration of intracellular probes. Light scattering, as well as the recently described cell staining, report characteristics that correlate with cell volume in a less direct way. Although radioactive methods could be included in the above categories, they are rarely used nowadays, and we only discuss them briefly at the end.

A note on terminology: we tried to make a distinction between "volume" and "size." Some techniques measure or attempt to measure cell volume proper, while others only generate parameters that correlate with cell volume. We try to reserve the word "size" for the latter type of measurements.

Liquid Displacement

When cells are placed in a small volume, the relative displacement of extracellular liquid by cell bodies can be significant and easily detectable. Four types of methods have been used for its detection: by a decrease in electrical conductance (Coulter method), by an increase in light transmission (when an absorbing dye is added to the medium), by a decrease in fluorescence (when a fluorophore is added to the medium) and by a decrease in hydraulic resistance.

Electric Conductance (Coulter Method)

Coulter electronic counting and sizing has become an essential tool for counting and characterization of various particles, including biological cells. The typical Coulter sizer has two compartments, each containing an electrode. One of these compartments is filled with a suspension of cells in an electroconductive fluid, such as any typical cell medium with salts; the other initially has a solution of a standard electrolyte. These two compartments are mostly insulated from each other by the material of the tube and are only connected by a 50–100 μm aperture in the tube wall. Thus, if a voltage is applied between the electrodes, the amount of electric current is limited by this narrow passage. When a dielectric cell passes through the aperture, the resistance between the compartments is further increased, in direct proportion to the amount of displaced solvent (which is equal to the volume of the particle). The increase in resistance is recorded by an electric circuit as a voltage spike (the instrument is operated in a constant current regime) and can be converted into the cell volume using calibration with standard beads. To force cells through the aperture at a steady rate, a negative pressure is applied to the tube, drawing the sample inside (and then removing it into a waste container).

Coulter sizing is widely used in hematology and microbiology and is often referred to as the "gold standard" against which other techniques are compared. The results are relatively independent of cell shape, and only an intact membrane is required. The measurable particles can be as small as 0.1 μm, but the latter depends on the aperture: a linear relationship between the signal and the particle volume is realized only for particle/aperture diameter ratios between 0.02 and 0.6. Thus, smaller apertures should be used for smaller cells, like bacteria, and larger apertures are better suited for larger mammalian cells.

In addition to measuring stable cells, the Coulter technique has been used extensively to study cell swelling and shrinkage in solutions with different salt concentrations (11–13). In this case, however, some caution is advised. The magnitude of the electric pulse depends on the conductivity of solution; accordingly, it was found that in less concentrated solutions, the apparent particle volumes increase (14; Yurinskaya et al. Submitted); others, have found, however, that diluting a 300 mOsm solution down to 225 mOsm had no effect on their data with beads (15). In any event, it seems that

running calibration beads in solutions identical to those used in cell studies would be a reasonable approach (16,17) and is in fact recommended by the instrument manufacturer.

Coulter sizers are made by Beckman Coulter (http://www.beckman.com/particle/instruments/cell-sizing-and-processing). A handheld version is available from EMD Millipore under the name Scepter Cell Counter (http://www.emdmillipore.com/US/en/life-science-research/cell-analysis/scepter-cell-counter/w2ib.qB.Ly4AAAE_Pc1kifKu,nav?cid = BI-XX-BSP-P-GOOG-SCEP-B325-1001). Electronic volume measurements have been also incorporated in some flow cytometers. One is the now-discontinued Cell Lab Quanta (Beckman Coulter). A sensing aperture suitable for cells up to 40 μm in size is made in these instruments in a shape of a flat channel. In addition to electronic measurements, a high-power objective simultaneously collects fluorescence from passing cells, and a 488 nm laser generates a side scatter signal. The still available Sony EC800 and SH800 analyzers operate in a similar manner.

Electronic measurements have been adapted for stationary cells in a microscopic setting. Cells were grown in a shallow chamber (18) or on a coverslip placed inside a shallow passage connecting two large fluid containers with electrodes (19). Cell swelling or shrinkage changed the cross section of the opening and, consequently, the electrical resistance.

More recently, a number of authors have realized the Coulter principle in microfluidic devices. In addition to the obvious advantages, such as reduced cost and the amount of sample, microfluidics makes it possible to control the cross section of sample flow using the technique of hydrodynamic focusing (20,21). It replaces the fixed apertures in standard instruments, which are prone to clogging. On the downside, quantification of cell volume on microfluidic Coulter devices is less straightforward. Modifications in electronics have been devised to improve the signal-to-noise ratio and particle discrimination (22). Electronic volume measurements can be combined with optical parameters (23).

Absorption

Cell volume measurements can utilize the displacement by intact cells of a strongly colored dye solution, with transmission image obtained at a wavelength of maximum absorption (24,25). Several dyes have been tested, but most work has been done using a food colorant Acid Blue 9 due to its low cost and apparent lack of effects on living cells at concentrations necessary to generate sufficient contrast ($\sim$0.7% with mammalian cells). Cells are placed in a shallow (up to 30–40 μm) chamber, which can be the space between a coverslip and a slide (kept separated by silicone grease), a slide with a shallow well, such as a sperm counting chamber, a perfusion chamber with a thin spacer (Bioptechs, PA) or a transparent cover with a recess that can be put over a cell culture dish (Scientific Device Laboratory, Des Plaines, IL). The sample is illuminated at 630 nm by means of a bandpass filter or an LED illuminator (Bioptechs or Ken-A-Vision, MO). Thicker cells appear brighter than the background in direct relationship to their thickness (Fig. 1a), while dead cells absorb the dye and turn dark. Cell volume is computed by first converting the image intensity into logarithmic units:

$$h = \frac{\ln I}{\alpha}$$

where α is the absorption coefficient of the medium. The cell volume is obtained by summation of the h values over the cell area and correcting for the background. Because of background correction, the results are insensitive to possible instability in the light source, and the method requires no calibration other than the knowledge of α; the latter can be obtained using the lens immersion method (28). The presence of the dye does not preclude the use of other transmission modes using blue illumination or simultaneous confocal or wide-field fluorescence, especially in the UV-to-blue range. Strong excitation by mercury lamp in the green range has to be limited to brief periods, as it may damage the samples; however, scanning with a low-power 547 nm HeNe line seems safe. When imaging rounded cells with high protein concentration, strong scattering may deflect some light away from the objective aperture, causing artefactual darkening; except in extreme cases, this can be corrected by taking control transmission images in blue light. The dye exclusion method has been applied to mammalian living cells (29–32), formaldehyde-fixed cells (33), bacteria (34). and protists (35). The method cannot be used for absolute volume measurements on confluent cultures, where the background intensity is unavailable.

Dye exclusion has been adapted to flow conditions in microchannels for blood cell analysis (36–38). Erythrocytes have a higher refractive index than most other mammalian cells, and to reduce the mentioned refraction/scattering artifacts, the authors added a high concentration of BSA to the medium (37).

Fluorescence

Fluorescence exclusion was first introduced for flow conditions (39); blood cells were suspended in a solution of membrane-impermeant fluorescent dextran and drawn into the analysis chamber of a flow cytometer. In the absence of particles, the sensing zone of the cytometer contained a uniform fluorescent solution of dextran surrounded by a nonfluorescent sheath fluid; if a cell is present, it excludes the volume of solution equal to its own volume, which should result in a decrease of fluorescence. Thus, the idea was to quantify the cell volume by a decrease in fluorescence associated with a passage of each cell. It turned out that the assumption of constancy of the stream diameter holds only so long as the latter is several times larger than the cell size; otherwise, a decrease caused by the particle is immediately followed by an increase, making these two signals hard to separate. Further investigation has shown that particles affect the distribution of the dye along the stream (40). Having a wider stream minimizes this problem but, conversely, results in a smaller relative displacement caused by a particle and a reduced signal/noise ratio. It is conceivable though that fluorescence displacement should work in a microcapillary that has no sheath fluid.

Becker and Fay sought to adapt the fluorescence exclusion method to microscopy (41). They had only a limited

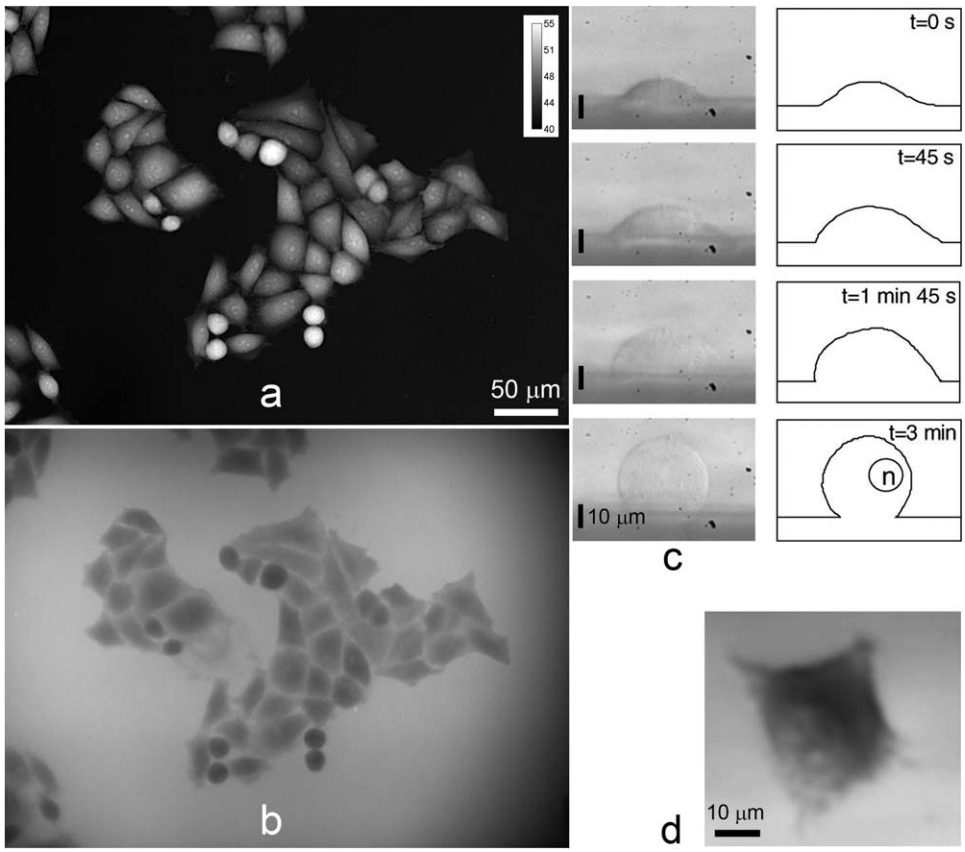

Figure 1. (a,b) HeLa cells imaged by transmission exclusion (a) and fluorescence exclusion microscopy (b). To obtain these images, a sample with live cells was mounted in a buffer containing both 6.25 mg/ml Acid Blue 9 (TCI America, OR) and 40 μg/ml CF488-dextran 10 kD (Biotium, CA) and observed using a 20×/0.75 objective. The transmission image (a) is shown on the logarithmic intensity scale, where local brightness is directly proportional to cell thickness in microns (shown by the calibration bar). There is a good overall correlation between the two images: those cells that are darker in fluorescence are brighter in transmission. The exception is the slightly darkened area between the two colonies on the fluorescence image, which has no counterpart in the transmission image. Panel (c) shows hypotonic cell swelling observed by side viewing. A sequence of images shows the changes of a cell side profile with outlines drawn in the right side. The volume increased by 80% at 45 s, 150% at 1 min 45 s, and $>$200% at 3 min; n indicates the nucleus [reproduced from Ref. 73, with permission from John Wiley & Sons, Inc.]. Panel (d) shows an acoustic image of a fibroblast, where elevated parts of the cell are shown as darker [reproduced from Ref. 108, with permission from Springer].

success because of photobleaching, as well as from unstable and spatially uneven illumination. However, the method has been given a second life in the hands of Bottier et al.(42), who used a more photostable conjugate of dextran and thoroughly tested the accuracy of results. Conversion of fluorescence intensity into cell height requires calibration, which can be achieved by placing the solution of dextran into wells of known depth or by immersing a spherical lens into the tested solution (43). Because alignment of the fluorescent lamp can affect calibration, the authors performed calibration for every experiment. Perhaps the main advantage of fluorescence exclusion over absorption is that nucleoli and other organelles with different refractive indices do not affect the height profiles, as they do in absorption (Fig. 1b); on the other hand, those short-range variations in absorption images do not compromise volume measurements because the lighter and darker areas caused by refraction cancel out during summation. The fluorescence method was later used by Gabella et al. (44), Zlotek-Zlotkiewicz et al. (45), and Jin and Verkman (46); the latter authors used it on a microfluidics chip.

Resistance to Flow

Slightly similar ideas lie behind a rather unusual method for cell volume measurements proposed by Davis et al. (47). The authors made use of the Poiseuille law, which states that resistance to fluid flow in a tube depends on the tube radius as $1/r^4$. Cells were grown in a glass capillary connected in series with a reference capillary, and various solutions were passed through this system. When cells changed their height in response to varying osmolarity, the effective radius of the lumen changed correspondingly. From the distribution of pressure between the two capillaries, cell volumes were calculated. The method requires somewhat unconventional handling of cells and may be subject to various caveats (such as the effect of variable cell confluency), but the authors were able to measure relative dynamic responses to osmotic challenges.

Geometrical Approaches

Cell Height (z Dimension)

Although representing cell volume with a single parameter of cell height may look very inadequate, it can be useful for studying rapid (i.e., osmotically induced) relative volume changes in dense layers, where cells are free to expand or shrink only vertically. In one method, ~1 μm fluorescent beads are introduced into the medium; some of them attach to the apical cell surfaces and others mark the bottom of the dish (14,48,49). Their vertical location is determined by maximum intensity in a wide-field of confocal fluorescence microscope, and changes in the distance between the top and bottom beads represent the relative changes in cell volume. A similar approach has been used with nonfluorescent beads (50).

The ingenious modification introduced by Kao and Verkman (51) improves the speed of measurement of the beads' z position. The focal plane remains fixed and, as the beads move up or down, their images become more blurry or less blurry, in accordance with the displacement. An additional cylindrical lens was introduced in the optical path to simplify conversion of the extent of blur into distance.

If electrophysiological equipment is available, one might consider using a glass microelectrode. Two variants of the method have been described. Roy and Sauvé (52) lowered the electrode to touch the cell surface; the dimple caused by a contact is visible under a phase contract microscope. The level where the electrode touches the membrane is compared to the level where it touches the bottom. Reproducibility of each measurement (membrane and bottom) was ± 0.5 μm (52). In addition to that, Kawahara et al. (53) used the sensitivity of electric current through a patch electrode when the latter is brought to within 3–4 μm of the cell surface. The idea behind their method resembles that of the ion conductance scanning microscopy (see below).

Some of the more time-consuming techniques described below, such as ion conductance (54), confocal (55,56) or side viewing (57), have been used sometimes only to monitor cell height, either at a single location or as a two-dimensional height profile. As previously mentioned, the neglect of the xy cell dimension seems justified in confluent layers or during rapid volume disturbances.

2D Cross Section (xy Dimension)

Measurements based on the cell's directly visible projection could be possibly traced back to the beginnings of microscopy. In their simplest variant, these methods are relatively straightforward and still used occasionally. Cells are assumed to be approximately spherical; their diameters d or cross-sectional areas are estimated and used to calculate the volume as $^1/_6\pi d^3$. Imaging is usually done in transmitted light (58–63) but fluorescence can also be used (64). It is obvious that representing even a loosely attached cell with a sphere (rather than a spheroid or some other shape) requires a certain leap of faith from the experimenter, and direct testing of cell sphericity is rarely done (65). [In fact, a spheroidal shape has been assumed for plant protoplasts in a microfluidics-based method (66)]. Even if a cell is spherical, care should be taken to only use its largest projection for volume estimation (67). Most papers that use this method provide little experimental detail; conversely, detailed investigations of image analysis techniques for automated detection of cell boundaries (a step which may be required to calculate the volume) are available (68,69).

Light Obscuration

A measure of the xy dimension can be obtained by the light obscuration technique. Detection of protein aggregates is the main biotechnological application of light obscuration, but it can be applied to cell analysis as well (70). A stream of particles flowing in a single file through a detection zone is illuminated by a laser, pointed directly at the detector. Each passing particle deflects some light from the detector and transiently attenuates the recorded signal; the size of the shadow cast by a particle roughly reflects its size.

Side Viewing (xz Dimension)

The method developed by Boudreault and Grygorczyk (57) can be called two-angle tomography. A specially designed perfusion chamber permits vertical mounting of a coverslip, enabling a side view of cells close to the edge of the coverslip (Fig. 1c). At the end of experiment, the coverslips are removed, and the same cells are viewed again, this time in normal orientation, to obtain their xy dimensions (later, the authors adapted a second camera to image both projections simultaneously). Two projections are not quite enough to fully reconstruct a three-dimensional shape, and certain assumptions have to be made. Although dynamic changes could only be observed from the side, the authors found that the attachment area remained unchanged in osmotic experiments and only cell height responded to osmolarity. This method has been used in subsequent publications from the Grygorczyk and Orlov labs (e.g., (26,71–73)).

Surface Scanning

If one knows the profile of the apical cell surface and, at the same time, if the basal surface is in tight contact with a flat substrate, cell volume can be calculated. Hence the rather numerous applications of atomic force microscopy (AFM) to cell volume measurements (74–80). AFM is usually used in the contact or in the tapping mode. In contact mode, the tip is being dragged along the cell surface in a raster pattern, and its vertical position is continuously recorded; from this information, an image of the surface is formed (81). In the tapping mode, the tip additionally oscillates at a constant frequency, and the surface is sensed by dampening of the oscillations. Cell measurements by AFM is a delicate undertaking because of the difficulties in following abrupt changes in cell height, such as between the cell body and the lamellipodium, and the possibility of a significant membrane deformation under the tip (76,78,80,82).

Scanning ion conductance microscopy is a relative new technique that utilizes the fact that electric conductance decreases in a close proximity to a nonconducting body (83). An electrode is moved along the surface without touching it

and maps the surface profile. As in AFM, image acquisition is slow: scanning of 64 points within a 30 × 30 μm area can take 2 min (83). Faster dynamic volume measurements may have to be based off cell height at a single point (54). A comparative study of ion conductance scanning and AFM has concluded that ion conductance is more accurate, and AFM tends to underestimate the cell volume (84). However, both types of imaging are prone to errors if a part of the cell's basal membrane recedes from the substrate.

Through-Focus Transmission Imaging

Bright-field microscopy can be used to obtain three-dimensional information about cell shape and volume by taking multiple images separated by small vertical steps, so that the object is effectively represented by multiple stacked discs (85,86). The area of each plane is measured, and the volumes of all optical discs are summated. However, bright-field imaging has a large depth of field, and out-of-focus parts of the image become superimposed on the in-focus plane. An improvement comes from using differential interference contrast (DIC) instead of bright-field because, like confocal imaging, DIC minimizes out-of-focus blur (87) and makes possible more accurate localization of cell boundary (69,88). The article by Phillips et al. (69) contains computer code for cell volume calculation from DIC stacks.

Correction for the vertical step size may have to be applied; that will be discussed in more detail in the next section.

Confocal Scanning

Confocal scanning might seem a natural choice for microscopy-based volume measurements because of its intrinsic depth sectioning ability. The technique requires demarcation of cell boundaries with a fluorescent stain. The fluorophore can be a cytosolic marker (89–93), a membrane marker (33,94,95) or a cell-impermeant dye that fills the extracellular space (56,96,97). Once such a sample is available, it is scanned at appropriately small vertical z-steps to determine the distance between the bottom and the top of the cell at every xy position. This provides all the information from which the volume can in principle be calculated. Confocal-based volume measurements are best done with high-NA objectives because those have better depth discrimination.

On closer inspection, application of confocal scanning to volume measurements is not very straightforward. The obvious problems are the slow speed of image acquisition, possible incompatibility of the fluorescent volume marker with other fluorescent probes that one might wish to use, and stability of staining. Additionally, one also has to be aware of the caveats specific to volume measurement. First, the step reported by the imaging software $\Delta z'$ (which can be the displacement of either the stage or of the objective) is not equal to the shift Δz_f of the focal plane within the sample. If the refractive index of the objective immersion medium n_i is smaller than that of the sample n_s (for example, when a dry objective is used with an aqueous sample), then $\Delta z_f > \Delta z'$, and the depth is underestimated. Conversely, the depth is overestimated when an oil-immersion objective is used with an aqueous sample. The simple correction formula that follows from geometrical optics is

$$\Delta z_f = \Delta z' \frac{n_s}{n_i}$$

This formula is undoubtedly correct for low-power objectives, but whether it is accurate for high-NA objectives is a matter of some controversy. Some authors have concluded that the formula is still accurate (98–101) but others have found deviations from linearity (102,103). Because the refractive index of cells and organelles is typically between 1.36 and 1.40, the use of water-immersion ($n_i = 1.34$) or silicone oil-immersion objectives ($n_i = 1.41$) would minimize the axial mismatch and make the correction unnecessary (104).

Even with high-NA objectives, the cell boundary is inevitably blurry, and some image processing (segmentation) must be applied to extract the thickness data from images. There is no universal method for cell segmentation, and the choice might depend on how the sample is stained, as well as on other factors, such as the extent of photobleaching during image acquisition (92,94,96).

Lastly, the local thickness data must be converted into volume data. Various algorithms for this operation have been published (96,105). Volume calculation on segmented images can be accomplished by commercial programs Imaris (www.bitplane.com), Amira (https://www.fei.com/software/amira-3d-for-life-sciences/), Voloom (https://micro-dimensions.com/voloom/) and ImageJ plugins Volumest (http://lepo.it.da.ut.ee/~markkom/volumest/) and Volume Calculator (http://imagej.net/Volume_Calculator). One can also carry out manual "integration" by summation of cell areas at each z-level multiplied by Δz (106).

Confocal scanning can be applied even to unstained samples using a stronger reflection from boundaries separating regions with different refractive indices (55). To increase acquisition speed, the authors used scanning within a single vertical plane. Because the difference in refractive indices between cells and the medium is small, the reflected signal from the apical side of the cell was rather noisy and required extensive processing, one cell image at a time. While cell biological applications of confocal reflection seem to present some challenges, the method is widely used in material analysis, where reflection intensities are much stronger.

Acoustic Microscopy

Acoustic microscopy is more common in the materials characterization field, but applications to biological cells seem to be on the rise (107). For this method, short pulses of acoustic wave are generated by a piezoelectric film and focused on the sample by a special lens; the latter may be immersed in the cell culture medium. The wave has to be of high frequency (up to 2 GHz) to obtain wavelengths short enough for imaging on the cellular scale. The wave is reflected from the cell surface, as well as from the underlying flat substrate; the difference in the arrival times between the apical echo and substrate echo gives cell thickness (Fig. 1d). The speed of sound in the cells can be assumed to be 1,560–1,570 m/s (27), which

is slightly higher than that in water (1,521 m/s) due to a high concentration of protein. Alternatively, one can use the echo reflected from the bare substrate in the vicinity of the cell, and use the speed of sound in water to calculate cell height. This method involves point-by-point imaging; measuring the volume of one cell takes approximately 5 s (108). Acoustic imaging has been used to study osmotic volume changes in cultured cells (109,110).

The other way to measure cell volume by acoustic microscopy is to observe the interference pattern between the waves reflected from the cell surface and from the substrate. The image consists of brighter and darker interference fringes that connect points of equal height; separation between adjacent minima and maxima correspond to the vertical distance of a quarter wavelength. Similar methods have been tested for optical waves (see references in (111)); however, the advantage of acoustic microscopy is a more predictable speed of wave propagation through the cell and a larger focal depth permitting imaging of the entire cell in a single shot. Lower resolution of acoustic images, compared to optical images, help mask irregularities in the cell attachment to the substrate.

An in-depth discussion of acoustic imaging can be found in the monograph by Briggs and Kolosov (107). Biological acoustic microscopes are currently available from Kibero (http://www.kibero.com/).

Quantitative Phase Imaging and Similar Techniques

There are some methods whose primary purpose may be different from measuring the cell volume but where the volume may come as an attendant result. The term "quantitative phase imaging" refers to a group of techniques that quantify the delay of a light wave passing through a sample (112–114). The phase delay $\Delta\varphi$ introduced by a cell is typically measured relative to that in the cell-free area; thus, $\Delta\varphi$ is proportional both to cell thickness h and to the refractive index difference between the cell and surrounding liquid:

$$\Delta\varphi = \frac{2\pi}{\lambda} h(n_{\text{cell}} - n_{\text{medium}})$$

For typical media used for cell culture, $n_{\text{medium}} \approx n_{\text{water}}$, and the difference $n_{\text{cell}} - n_{\text{water}}$ is proportional to intracellular concentration C of optically dense organic compounds; inorganic salts have practically no effect on the refractive index. The quantitative relationship between Δn and C is approximately (115)

$$n_{\text{medium}} - n_{\text{water}} \approx 0.2C(\text{g/ml})$$

Thus, $\Delta\varphi$ integrated over the cell area A reflects the total amount T of organic material contained in the cell:

$$\sum_{\text{A}} \Delta\varphi = \frac{2\pi}{\lambda} V \Delta n_{\text{average}} \approx \frac{2\pi}{\lambda} V \cdot 0.2C = \frac{2\pi}{\lambda} \cdot 0.2T$$

The subscript "average" indicates that, for the purpose of cell volume calculation, the cell can be represented by a single averaged refractive index.

Monitoring cell growth by accumulation of organic material is one direct application of quantitative phase imaging (116). In addition, quantitative phase imaging can be used to reconstruct three-dimensional cell shape (under the assumption of a uniform n_{cell}) or to measure cell volume, but the latter would require independent knowledge of the refractive index. In reality, it is more common to separately measure $\Delta\varphi$ and V (e.g., by one of the previously described methods) and use those to find n_{cell} (117).

It follows from the last equation that $\Delta\varphi$ is not affected by intracellular water under normal experimental conditions. This point is essential because the distinction between integrated phase (which is sometimes called the "optical volume") and the physical volume is not always clearly enunciated in the literature or in commercial information. Despite this almost inherent limitation of phase imaging, several authors came up with special ways to incorporate cell thickness into the technique by modifying the extracellular liquid.

Digital Holography

In the variant of quantitative phase imaging known as digital holography, the illuminating beam is split into the object beam that crosses the sample and the reference beam that bypasses the sample. These beams are recombined past the objective and form an interference pattern that carries information about the phase delay $\Delta\varphi$; the phase can be recovered by means of computer processing. Commercial holographic microscopes are available from Lyncée Tec (http://www.lynceetec.com/), PHI (www.phiab.se), Tescan (http://www.tescan.com/technology/light-microscopy/q-phase) and Ovisio (http://www.ovizio.com/).

The phase delay introduced by a cell still remains a product of two unknowns, V and $\bar{\Delta n}$. In several publications by Marquet, Rappaz and their collaborators, a method of extracting cell thickness from the phase data has been developed. It is based on the notion that when two phase measurements of the same object are performed in liquids with different n_{medium}, one obtains two equations with two unknowns, V and n_{cell}, which then can be easily solved. In one implementation of this idea (94,118), the authors used consecutive perfusion of a sample with two isosmotic solutions that differed slightly in their refractive indices. Subsequently, the authors made use of the fact that if a medium contains a dye with a large extinction coefficient, the refractive index becomes strongly wavelength-dependent in the vicinity of the absorbance peak. Thus, they added a dye to the medium and probed the sample not with one but with two monochromatic beams with wavelengths located at different distances to the absorption peak. For the dye, they first used 30 mM sulforhodamine B1 with a peak absorbance at 565 nm (119) but later found a more cell-compatible dye, 20 mM Fast Green FCF (625 nm) (120).

Clearly, as a standalone approach to cell volume measurement, holographic microscopy would be unnecessarily complicated, but if one is interested in the refractive index as well, the double-beam method kills two birds with one stone.

Perfusion with an Optically Dense Medium

A different approach was put forth by Verkman and coworkers (121,122). Consider a cell in contact with a medium, which contains an optically dense material, such as 5% dextran. If the medium becomes hypertonic (for example) with respect to the cell, some water will pass from the cell into the medium. This will cause cell shrinkage and medium expansion, but the total amount of optically dense matter will remain unchanged; simple transfer of water between the cell and the medium is not detectable by phase imaging. Suppose, however, that we additionally keep replacing the medium with a fresh one. The enlarged volume occupied by the medium will now contain more dextran because the water that left the cell has been flushed out. This is the situation that does result in a change of phase; in effect, it is not the change in the cell volume but a change in the extracellular volume that is being measured.

This method was first applied to imaging with a Mach-Zehnder interference microscope (121), which utilizes an optical path similar to that in a digital holographic microscope. Such microscopes are no longer available commercially, but the idea might be applicable to holographic imaging as well. In the next publication, the authors adapted it to a much more common phase contrast imaging (122).

Optical Diffraction Tomography

Compared to digital holography, an optical tomographic microscope additionally illuminates the sample from different angles, by turning either the sample (123) or the beam (124,125). In tomography, no additional "tricks" are needed to achieve the decoupling of refractive index and volume. It seems, however, that quantitative accuracy of optical diffraction tomography has not been convincingly demonstrated as yet, and the results might depend both on the size and the refractive index of cells under observation (P. Marquet, Personal communication). A different type of three-dimensional restoration called Spatial Light Interference Microscopy has been developed by the Popescu group (126); the commercial instrument is available through Phi Optics Inc. The technique utilizes a phase contrast objective and includes additional optics for changing the phase between direct light and light scattered by the sample. The sample is scanned vertically in small increments, followed by extensive image processing.

For the sake of completeness, soft X-ray tomography may be mentioned. It has been used for characterization of organelles in frozen samples (http://www.bioopticsworld.com/articles/print/volume-6/issue-2/features/whole-cell-tomography-molecular-biology-structural-biology-affo.html; 127) and, at the same time, provides information on the cell volume (128).

Relative Changes in Cell Volume by Intracellular Volume Markers

Electrodes

Unlike most of the previously discussed methods where the entire cell is measured, intracellular volume markers are only sensitive to the amount of intracellular water (presumably to its osmotically active fraction). These methods are based on detecting concentration changes of an intracellular membrane-impermeant chemical. An increase in the cell volume causes dilution of the chemical, and vice versa. The idea was first demonstrated by L. Reuss on gallbladder epithelium loaded with tetramethylammonium (129). The cells were then impaled with a microelectrode sensitive to this ion, and, as the cell volume changed in response to external osmolarity, the recorded voltage changed correspondingly. This method was later used by Alvarez-Leefmans et al. (130), Adorante (131), and Dierkes et al. (132) and reviewed (2).

Fluorescence

More recently, fluorescence detection methods gained popularity as they are much easier than the use of electrodes. Membrane-permeant acetoxymethyl (AM) esters of various fluorophores can be loaded into cells, where the AM group is hydrolyzed by intracellular esterases, and the fluorophore becomes trapped inside the cell. When cells swell or shrink, changes in the fluorophore concentrations translate into local cell brightness. At sufficiently low fluorophore concentrations, fluorescence collected from a fixed volume should be proportional to the amount of fluorophore contained in that volume, that is, to its concentration. In this case, the appropriate fluorescence detection techniques would be those that sample a small volume within a cell; the *total* cell-associated fluorescence is expected to remain constant (which, as we will see shortly, is not necessarily true).

The approach based on local fluorescence was initially applied to the pH-sensitive dye BCECF and the Ca^{2+} indicator Fura-2 (with the second goal of measuring pH and calcium along with the volume). Fluorescence readings for volume measurements were taken at isosbestic points, where fluorescence is insensitive, respectively, to pH or to Ca^{2+} (14,133,134). The authors, however, used regular wide-field illumination in those experiments, which has a very limited sectioning capacity and tends to collect the entire fluorescence from the sample (135). Subsequently, the fluorescent dye calcein became more popular due to its superior brightness and insensitivity to ions and to pH; by closing the field diaphragm to restrict illumination to a small spot, sensitivity to the local concentration of the fluorophore was improved (136). Nowadays, confocal microscopy is widely available and provides a more natural way to achieve depth selectivity (90). Total Internal Reflection Fluorescence (TIRF) is equally effective because it excites fluorescence only within a thin slice next to the basal membrane (137); both confocal scanning and TIRF continue to be used (138,139). One limitation of the calcein method has been immediately pointed out by its inventors: part of the trapped fluorophore becomes compartmentalized and does not respond to volume changes (136). Indeed, comparison with height measurements suggested that fluorescence trapping may underestimate changes in the total cell volume (14).

In a separate line of development, investigators sought to make use of the self-quenching properties of fluorophores. It is well known that, for some fluorophores, including calcein, the dependence of local fluorescence intensity on the fluorophore concentration is bell-shaped: the initial linear increase

gives way to a decrease caused by interactions between molecules. In other words, at low concentrations, the fluorescence from each molecule (quantum yield) remains constant, but at higher concentrations, individual molecules begin to quench each other, and the quantum yield decreases. The advantage of using the declining phase of the curve is that the entire cell-associated fluorescence is affected, and not just the local fluorescence density. That makes depth discrimination unnecessary, and spectrofluorometers or microscope objectives with low numerical apertures are adequate for such measurements.

One of the early applications of calcein quenching was the investigation of glucose transport in erythrocyte ghosts (140); subsequently, various authors began applying it to cells. Wehner et al.(141) and Werner and Tinel (142) used a laser scanning confocal microscope (which is not required in the case of quenching but is certainly possible) to observe changes in intracellular calcein fluorescence that were opposite to volume changes. Hamann et al. (143) undertook a more detailed study of the calcein quenching method. By repeatedly microinjecting calcein into retinal epithelial cells, the authors first observed an increase and then a decrease in fluorescence. Accordingly, swelling produced a slight increase and shrinkage produced a slight decrease of fluorescence in their osmotic experiments. Concentration-dependent quenching of BCECF has also been observed (144).

Thus, it appears that sometimes, shrinkage causes an increase in local calcein fluorescence (as one would expect from its increased concentration) and other times it causes a decrease in fluorescence (as one would expect if self-quenching was a factor). Whether this discrepancy is related to various degrees of calcein loading is not entirely clear: besides the qualitative microinjection experiments of Hamann et al. (143), the relationship between quenching and loading has only been observed in Madin-Darby Canine Kidney (MDCK) cells (17). However, Precourt (145) noticed that exposure of MDCK cells to 4 μM calcein AM for 80 min resulted in intracellular concentrations of no more than 20–30 μM, which is still two orders of magnitude less than required for self-quenching. A plausible resolution to this quandary was offered by Solenov et al. (146), who showed that quenching of intracellular calcein can be concentration-independent and suggested that it is mediated by cytosolic proteins. If this is the case, shrinkage should always cause a decrease in the quantum yield, but this effect may or may not be offset by an increase in the fluorophore concentration; swelling would do the opposite. Thus, inconsistencies in calcein behavior now receive a simple explanation, and, indeed, the effect of imaging conditions on the apparent behavior of calcein was directly demonstrated by Davidson and Higgins (147). The use of calcein in the quenching mode remains popular due to the fast responsiveness of the method (148–150). If the behavior of calcein in a particular cell type is known, conversion of fluorescence into cell volume is possible (151), but typically, calcein-based measurements are only expected to produce semiquantitative results.

At least one other fluorophore has been tried for volume measurements. Srinivas and Bonnano (152) have observed quenching of the dye 6-methoxy-N-(3-sulfopropyl)-quinolinium (SPQ) by cytosolic proteins or by some other unidentified intracellular quenchers. The usefulness of SPQ as a volume sensor is limited due to sensitivity of its fluorescence to chloride.

Chloride

Chloride, however, can be used as a volume sensor in its own right. Unlike calcein, it cannot be regarded as necessarily trapped inside the cell but, being the most abundant intracellular inorganic anion, it is intimately related to cell volume (153). To illustrate the concept, suppose that a cell is placed in a solution with higher osmolarity, and a new osmotic equilibrium is established. Three situations can be considered. (1) If the membrane were impermeable to chloride (or if an early response was observed, before chloride had time to redistribute), chloride is essentially trapped, and osmotic shrinkage would produce a corresponding increase in chloride concentration. (2) Many cells undergo the so-called regulatory volume increase (RVI) following an initial efflux of water. It is brought about by opening of ion channels and by entry of chloride and sodium into the cell (153). Thus, the new cell volume, which is equal or smaller (in the case of incomplete RVI) than the initial volume, will contain an extra amount of chloride, and its concentration will be higher than before the disturbance. (3) To predict chloride concentration changes during RVI, we may consider the state of equilibrium in a more quantitative manner by writing out two equations:

$$z[\mathrm{M}] + [\mathrm{Cl}] = [\mathrm{K}] + [\mathrm{Na}]$$
$$[\mathrm{M}] + [\mathrm{Cl}] + [\mathrm{K}] + [\mathrm{Na}] = \mathrm{P}$$

The first equation expresses electrical neutrality within the cell and the second is a simplified condition of osmotic balance (154). In these equations, square brackets denote intracellular concentrations, M stands for negatively charged organic osmolytes with average valency z, and P is the external osmolarity; inorganic anions other than chloride are neglected. We assume that the total amount of organic osmolytes M_T is conserved. By expressing $[M]$ through cell volume as M_T/V and rearranging, we obtain a formula for chloride concentration:

$$[\mathrm{Cl}] = \frac{P}{2} - \frac{M_T(z+1)}{V}$$

During RVI, P remains constant and cell volume V is increasing; therefore, chloride concentration should be increasing as well. The opposite changes are expected to take place in a hypoosmotic solution. In the case of apoptotic dehydration, which occurs under conditions of constant osmolarity, shrinkage should be accompanied by a decrease in chloride concentration.

Thus, chloride can be used as a reporter of relative changes in cell volume, especially during rapid processes, and this has been demonstrated in at least two publications (155,156). Lately, genetically engineered sensors based on yellow fluorescent protein have become the preferred tool for intracellular chloride measurements (157,158). Despite their many advantages over chemical chloride probes, they suffer

from sensitivity to pH. However, in the chloride-sensitive protein named clophensor, this sensitivity has been turned into advantage by enabling double Cl^--pH detection at two wavelengths (159).

Indirect Methods: Light Scattering and Cell Staining

Optical elastic scattering (the word "elastic" indicates that the frequencies of illuminating and scattered waves are equal) is widely used in biological applications (160). Light is scattered by all particles whose refractive index is different from that of the environment; because, as a rule, larger particles scatter stronger, the scattering intensity may carry information about the particle size. However, the intensity and the angular distribution of scattering depend not only on the particle size, but also on its shape, roughness, refractive index, and the presence of organelles (161). Moreover, scattering intensity can be strongly angle-, wavelength-, and polarization-dependent (162,163). Because of all these complexities, scattering methods do not achieve volume quantification in absolute units. While large differences in cell size are usually easily detectable, smaller changes, especially when accompanied by changes in the cell shape, structure or water content, may affect the scattering intensity in unpredictable ways. As far as volume measurements are concerned, one important advantage of scattering is that it responds to volume changes practically instantaneously, which can be valuable for kinetic studies.

Light Scattering in Flow Cytometry

The dependency of scattering on the particle size is used extensively in flow cytometers. All standard flow cytometers are equipped with two detectors of scattered light: one is positioned at a small angle (0.5°–2°) to the incoming beam (forward scatter or FSC) and the other collects light at 15–135 degrees (side scatter or SSC; (164)). Experiments with beads have shown that the FSC signal generally increases with bead size (though not always monotonically; (165,166)). For reasons already mentioned, the situation with cells is more complicated. By comparing flow cytometric parameters with electronic sizing data, Tzur et al. (164) concluded that SSC, FSC and autofluorescence all correlate with cell size, but no single parameter can serve as a universal measure of cell volume. For red blood cells that have no internal structure and were treated to become spherical, it was possible to obtain accurate data on volume and hemoglobin concentration (167). Platelets with average volumes $\sim$10 μm^3 are about the smallest cells that can be resolved by light scatter (168).

The outcome of scattering measurements may depend on the exact cause of variability of cell volume. The experiments by Tzur et al. (164) were performed on uniform populations, where cells differed only in their position in the phase cycle. Cell water content remains relatively stable in many cell types throughout the cycle (32,169,170), and therefore, the cell size may have been the main variable in those experiments. However, in many applications of cell volume measurements, preservation of the refractive index cannot be assumed. Such are the experiments where cells are exposed to anisosmotic media: hypoosmotic solutions cause cell swelling with a concomitant decrease in the refractive index and hyperosmotic conditions have the opposite effect. A brief survey of the literature shows that osmotically induced changes in scattering intensity can behave in many different ways. A good correlation between electronically measured volume and FSC has been reported for sperm (171) and for neutrophils in hypotonic conditions (172). However, Keller et al. (173) found no correlation between FSC and the electronic volume of activated neutrophils. In other studies, FSC varied inversely with cell volume for neutrophils and other cell types (174). The latter effect has been given a theoretical explanation that considered the relative contributions of the refractive index and cell size to the scattering properties of osmotically perturbed cells (175). Thus, it seems that if flow cytometric scattering is to be used in osmotic experiments at all, it should be thoroughly validated for a particular set of conditions.

Flow cytometry has also been used to assess the characteristic cell shrinkage during apoptosis (176): apoptotic cells are expected to have a reduced FSC due to their smaller size and an increased SSC due to a higher refractive index. However, not all apoptotic cases conform to this pattern (177), and, just as with osmotic experiments, a complex interplay between refractive index, size, shape and instrumental factors may confound the interpretation of scatter plots ((178); Yurinskaya et al. Submitted).

Light Scattering in Suspensions

The method of detecting changes in cell volume by light passing through a cell suspension has been used as early as the 1930s. The experimental situation here is different from scattering on single cells because light can undergo multiple reflections and refractions on its way to the detector. The two simplest configurations use front detectors (as in absorption spectrometry) or side detectors (as in fluorescence spectrometry); additionally, stopped-flow can be used to better resolve the first moments of osmotic swelling or shrinkage (179,180). Because extended light sources, such as halogen lamps, were used in the early transmission experiments, the detectors probably captured both direct transmission and low-angle scattering. It has been consistently found that the amount of light passing through a cell suspension decreases when cells shrink and increases when they swell under anisosmotic conditions (65,181–183). Interestingly (and somewhat counterintuitively), the right-angle scattering responded to osmotic disturbance similarly (184–186). Given that scattering from cell suspensions may depend on numerous cell- and instrument-specific parameters (187), these results should be generalized with caution.

Light Scattering in Microscopy

Similar principles have been applied in a microscopic setup (49,188–190). Cells were grown on coverslips to a high density and illuminated with a tungsten-halogen lamp or a laser beam; various placements of light detectors have been tried. As with other implementations of scattering techniques, the results are difficult to summarize. For example, the same

Table 1. A rough comparison of the methods discussed in this article

METHOD	STATE OF CELL ATTACHMENT	ACCURACY	TYPE OF MEASUREMENTS	SPEED	CUSTOM DEVICES	INSTRUMENT
Coulter	Suspended	+++	Absolute	++		Coulter analyzer
Exclusion (absorption)	Any type	+++	Absolute	++	Minimal	Light transmission microscope
Exclusion (fluorescence)	Any type	+++	Absolute	++	Minimal	Fluorescence microscope
Resistance to flow	Attached	+	Relative	++	Yes	Pressure gauge
Cell height	Attached	+	Absolute	++		Fluorescence microscope
Cell area	Loosely attached	+	Absolute	+++		Light transmission microscope
Side viewing	Attached	++	Absolute	+++	Yes	Light transmission microscope
Surface scanning	Tightly attached	++	Absolute	+		Atomic force microscope
Surface scanning	Tightly attached	+++	Absolute	+		Scanning ion conductance microscope
Vertical sectioning	Attached	+++	Absolute	++		Confocal or DIC microscope
Acoustic	Attached	++	Absolute	++		Acoustic microscope
Digital holography (two-beam)	Attached	++	Absolute	+++	Yes	Digital holographic microscope
Interferometry	Attached	++		++	Maybe	Mach-Zehnder microscope
Optical tomography	Attached	++	Absolute	+		Spatial Light Interference microscope
Volume markers (concentration)	Attached	++	Relative	+++		Confocal or TIRF microscope
Volume markers (quenching)	Any type	++	Relative	+++		Fluorescence microscope or spectrometer
Volume markers (chloride)	Any type	++	Relative	+++		Fluorescence microscope
Light scattering	Suspended	Variable	Relative	+++		Flow cytometer, spectrometer
Light scattering	Attached	Variable	Relative	+++	Yes	Custom microscope
Molecular staining	Any type	++	Relative	slow		Various
Radioactive	Any type	Unknown	Absolute	slow		Radioactive counter

The evaluations given to each method are very approximate and can be subject to many conditions and variables.

group first reported an increase (188) and later a decrease (189) in scattering from cells swollen in hypotonic solutions. The plating density affects the cell shape and introduces another variable specific for scattering microscopy (189). The intensity of SSC can vary dramatically within as little as 1–2 degrees (191). However, once a successful experimental setup is found, responses to as little as 1% osmolarity change can be detected (192).

Molecular Staining for Mass Cytometry

Mass cytometry is a recently introduced technique, in which single cells are labeled with antibodies carrying heavy metal isotopes instead of fluorescent tags. The cells are vaporized, and the isotopes are quantified by mass spectrometry (193). The advantage of mass cytometry over flow cytometry is the reduced spectral overlap between different labels, permitting analysis of forty antigens simultaneously. However, unlike flow cytometric light scattering, there is no measurable parameter that would reflect cell volume.

In a recent publication, Stern et al. (194) showed that the lipid stain osmium tetroxide (which is detectable on a mass cytometer) correlates with forward light scatter and can be used as a proxy for cell size. There is of course no guarantee that the amount of lipids would always be proportionate to cell volume and, indeed, eosinophils exhibited disproportionately strong staining compared to other blood cell types. Nevertheless, osmium staining should be able to discriminate among cells with significantly different sizes or between different stages of cell growth.

Not only osmium tetroxide, but many other measures of molecular abundance may correlate with cell volume. In the same work, the authors demonstrated the utility of fluorescent wheat germ agglutinin, a protein that binds to N-acetyl-D-glucosamine and sialic acid residues, as a correlate of cell size. It would be interesting to test some more nonspecific stains in this capacity, such as the amino group reagent carboxyfluorescein succinimidyl ester.

Radioactive Methods

Dividing the directly measurable volume of a cell pellet obtained by centrifugation by the number of cells seems almost straightforward. The main problem is to carefully account for the gaps between cells. The details of the protocol

can be found in the papers by Savitz et al. (195), Bratbak and Dundas (196), or Kubitschek and Friske (197). A cell-impermeant marker of extracellular fluid, such as radioactively labeled inulin or albumin, is added to the suspension, and from the radioactivity of the pellet, the amount of extracellular fluid contained in it can be calculated. The volume occupied by cells in the pellet is found as the difference between the total volume of the pellet and the volume occupied by extracellular fluid.

If a chemical is distributed passively between the cell and environment, its cell-associated amount can be used to measure the volume of intracellular water. It is important of course to verify that the probe does not stick to any cellular components. In one work (198), ^{14}C-labeled nonmetabolizable sugar, 3-O-methyl-D-glucose, was used as an intracellular probe for cells grown in a monolayer. Hexoses enter cells by facilitated diffusion (except in kidney and intestine) until their intracellular concentration becomes equal to the extracellular concentration. After equilibration is reached, the cells are rinsed with a buffer containing phloretin, an inhibitor of sugar transport, before counting radioactivity and measuring protein.

This method may not be suitable for every cell type, and in another work (199), the authors used radioactive urea as a marker of intracellular space. Because the efflux of urea cannot be inhibited during washing, radioactive sucrose was added to quantify extracellular space. Intracellular volume was determined as the difference between the total volume (indicated by urea) and extracellular volume indicated by sucrose.

Effect of Cell Detachment and Fixation

When a Coulter analyzer is available, it can be tempting to apply it to attached cells by trypsinizing them and bringing into suspension. Although little research has been done on the effects of this procedure on cell volume, it is known that the state of attachment can profoundly influence cell volume regulation (14). Our unpublished data show that cell detachment may produce transient but significant changes in cell volume, both in the direction of shrinkage and swelling. Weiss (200) observed an unexplained loss of dry mass in Sarcoma 37 cells following exposure to 0.25% trypsin (a typical concentration used for cell culture treatment). Mallucci et al. (201) reported a rapid and dramatic volume increase (both due to protein synthesis and water intake) on exposure to only 1 μg/ml of trypsin. Although very limited, these data strongly suggest that cell detachment before volume measurements is undesirable, and adherent cultures should be analyzed in their original state.

The same can be said about chemical fixation. Scanning or transmission electron microscopy can significantly underestimate cell size because of shrinkage during specimen preparation (202,203). Formaldehyde fixation can cause either shrinkage or swelling of cells (33,204–206).

Summary

Methods of volume measurement can be characterized by their speed, accuracy, sensitivity, and whether they detect absolute or relative volume changes. The speed of measurement has two aspects: the amount of time required for a single measurement and, in some cases, the time needed to deliver a stimulus (e.g., an anisosmotic solution) to cells to initiate volume change. For example, confocal scanning can be relatively slow in obtaining a single reading, but it can be performed in an open dish where a stimulus can be easily added. By contrast, data acquisition in absorption or fluorescence exclusion is fast, but the sample has to be kept within a constricted space where rapid fluid exchange would require special arrangements. Microfluidics holds much promise in this regard.

The accuracy strongly depends on the type of sample. For example, AFM can easily detect submicrometer features on the membrane but it would be useless for measuring rounded cells. In principle, the best way to test for accuracy would be to apply a method to biological cells with known dimensions, but such cells hardly exist. It is common to use plastic beads for calibration, but not all methods are expected to work on beads and cells in the same way. It seems from available evidence that volume exclusion methods and confocal imaging corrected for refractive index mismatch can achieve good accuracy.

Sensitivity is easier to evaluate than accuracy because one can observe the response to a known small change in external osmolarity or to characterize the reproducibility of repeated measurements on the same sample. Sensitivity and speed are particularly important when cell volume is used as a readout of membrane channel function (even if the method only reports relative volume changes). For example, if one needs to screen for inhibitors of aquaporins or monovalent ion channels, it may be sufficient to compare the initial rate of volume change in the presence and in the absence of the tested chemicals (139,156,180). A number of methods described in this review, such as intracellular fluorescent sensors or many of the scattering techniques, have been developed with such applications in mind.

However, as with all uncalibrated techniques, direct comparison of results obtained on different instruments, at different times or on different sample preparations may be problematic. When rapid kinetics on a second time scale is not required, volume exclusion methods may provide the most accurate data. Those methods, however, rely on having an intact membrane. Cells that have been treated with detergents or chemical fixatives can be analyzed by methods based on bright-field or DIC microscopy.

Technologically demanding techniques, such as digital holography and tomography, do not seem to offer immediate advantages for volume measurements but they provide additional information, which may be valuable for certain applications. For example, in some cases, one may wish to quantify the individual contributions of water and dry mass to total cell volume; in these cases, absolute data on cell volume must be complemented by measurements of water concentration or

an equivalent parameter (32). Quantitative phase imaging then becomes an attractive option.

Table 1 provides a rough summary of the main methods. Their ranking, however, depends on many factors and can easily be misleading. The readers are advised to consult the text and the original literature.

Acknowledgments

The author gratefully acknowledges information and clarifications provided by Carl Bortner (NIH/NIEHS), Calvin Cotton (Case Western Reserve University, Cleveland), Jorge Fischbarg (Columbia University, New York), Ryszard Grygorczyk (University of Montreal), Jinseok Heo (Buffalo State College, New York), Estrella Hernandez (Beckman Coulter), Douglas Kline (Kent State University, Ohio), Robert Lemor (Kibero), Pierre Marquet (École Polytechnique, Lausanne), Kevin Phillips (Urology Diagnostics), Gabriel Popescu (University of Illinois At Urbana-Champaign), Paul Robinson (Purdue University, West Lafayette, IN), Howard Shapiro (Shapiro Lab) and Alan Verkman (University of California, San Francisco). The draft of this article was read by Robert Clements and Nathan Mudrak (Kent State University, Ohio) and Alexey Vereninov (Institute of Cytology, Saint Petersburg), who suggested valuable improvements. The author also thanks the journal reviewers for insightful comments. The work was supported by Kent State University Research Council.

Disclaimer

The author holds a patent on the cell volume measurement method based on exclusion of an absorbing dye.

Literature Cited

1. Macknight ADC, Leader JP. Volume regulation in epithelia: Experimental approaches. Methods Enzymol 1989;171:744–792.
2. Alvarez-Leefmans FJ, Altamirano J, Crowe WE. Use of ion-selective microelectrodes and fluorescent probes to measure cell volume. Methods Neurosci 1995;27:361–391.
3. Kimelberg HK, O'Connor ER, Sankar P, Keese C. Methods for determination of cell volume in tissue culture. Can J Physiol Pharmacol 1992;70:S323–S333.
4. Reuss L, Cotton CU, Altenberg GA. Measurement of epithelial cell volume. In: Wills NK, Reuss L, Lewis S, editors. Epithelial Transport: A Guide to Methods and Experimental Analysis. London: Chapman & Hall; 1996. pp 167–189.
5. Verkman AS. Optical methods to measure membrane transport processes. J Membr Biol 1995;148:99–110.
6. Verkman AS. Water permeability measurement in living cells and complex tissues. J Membr Biol 2005;173:73–87.
7. Narhi LO, Jiang Y, Cao S, Benedek K, Shnek D. A critical review of analytical methods for subvisible and visible particles. Curr Pharm Biotechnol 2009;10:373–381.
8. Hoffmann EK, Lambert IH, Pedersen SF. Physiology of cell volume regulation in vertebrates. Physiol Rev 2009;89:193–277.
9. Lang F. Mechanisms and significance of cell volume regulation. J Am Coll Nutr 2007;26:613S–623S.
10. Orlov SN, Platonova AA, Hamet P, Grygorczyk R. Cell volume and monovalent ion transporters: Their role in cell death machinery triggering and progression. Am J Physiol Cell Physiol 2013;305:C361–C372.
11. Civan MM, Peterson-Yantorno K, Coca-Prados M, Yantorno RE. Regulatory volume decrease by cultured nonpigmented ciliary epithelial cells. Exp Eye Res 1992; 54:181–191.
12. Roman RM, Wang Y, Lidofsky SD, Feranchak AP, Lomri N, Scharschmidt BF, Fitz JG. Hepatocellular ATP-binding cassette protein expression enhances ATP release and autocrine regulation of cell volume. J Biol Chem 1997;272:21970–21976.
13. Morales-Mulia M, Pasantes-Morales H, Morán J. Volume sensitive efflux of taurine in HEK293 cells overexpressing phospholemman. Biochim Biophys Acta 2000;1496: 252–260.
14. Raat NJ, De Smet P, van Driessche W, Bindels RJ, Van Os CH. Measuring volume perturbation of proximal tubular cells in primary culture with three different techniques. Am J Physiol 1996;271:C235–C241.
15. Hendil KB, Hoffmann EK. Cell volume regulation in Ehrlich ascites tumor cells. J Cell Physiol 1974;84:115–125.
16. Kulkarni SB, Sauna ZE, Somlata V, Sitaramam V. Volume regulation of spermatozoa by quinine-sensitive channels. Mol Reprod Dev 1997;46:535–550.
17. Fenton RA, Moeller HB, Nielsen S, de Groot BL, Rützler M. A plate reader-based method for cell water permeability measurement. Am J Physiol Renal Physiol 2010; 298:F224–F230.
18. Mazzoni MC, Lundgren E, Arfors KE, Intaglietta M. Volume changes of an endothelial cell monolayer on exposure to anisotonic media. J Cell Physiol 1989;140: 272–280.
19. O'Connor ER, Kimelberg HK, Keese CR, Giaever I. Electrical resistance method for measuring volume changes in monolayer cultures applied to primary astrocyte cultures. Am J Physiol 1993;264:C471–C478.
20. Oskui SB, Grover WH. Measuring the physical properties of cells. In: Lagally E, editor. Microfluidics and Nanotechnology: Biosensing to the Single Molecule Limit. Boca Raton, FL: CRC Press; 2014. pp 106–130.
21. Zheng Y, Nguyen J, Wei Y, Sun Y. Recent advances in microfluidic techniques for single-cell biophysical characterization. Lab Chip 2013;13:2464–2483.
22. Guo J, Ai Y, Cheng Y, Li CM, Kang Y, Wang Z. Volumetric measurement of human red blood cells by MOSFET-based microfluidic gate. Electrophoresis 2015;36: 1862–1865.
23. Holmes D, Pettigrew D, Reccius CH, Gwyer JD, van Berkel C, Holloway J, Davies DE, Morgan H. Leukocyte analysis and differentiation using high speed microfluidic single cell impedance cytometry. Lab Chip 2009;9:2881–2889.
24. Model MA. Imaging the cell's third dimension. Microsc Today 2012;20:32–37.
25. Model MA. 2015. Cell volume measurements by optical transmission microscopy. Curr Protoc Cytom 2015;72:12.39.1–12.39.9.
26. Platonova A, Koltsova SV, Hamet P, Grygorczyk R, Orlov SN. Swelling rather than shrinkage precedes apoptosis in serum-deprived vascular smooth muscle cells. Apoptosis 2012;17:429–438.
27. Pasternak MM, Strohm EM, Berndl ES, Kolios MC. Properties of cells through life and death - An acoustic microscopy investigation. Cell Cycle 2015;14:2891–2898.
28. Model MA, Khitrin AK, Blank JL. Measurement of the absorption of concentrated dyes and their use for quantitative imaging of surface topography. J Microsc 2008; 231:156–167.
29. Gregg JL, McGuire KM, Focht DC, Model MA. Measurement of the thickness and volume of adherent cells using transmission-through-dye microscopy. Pflugers Arch 2010;460:1097–1104.
30. Kasim NR, Kuželová K, Holoubek A, Model MA. Live fluorescence and transmission-through-dye microscopic study of actinomycin-induced apoptosis and apoptotic volume decrease. Apoptosis 2013;18:521–532.
31. Gibbons BA, Robinson LC, Kharel P, Synowicki RA, Model MA. Volume measurements and fluorescent staining indicate an increase in permeability for organic cation transporter substrates during apoptosis. Exp Cell Res 2016;344: 112–119.
32. Mudrak NJ, Rana PS, Model MA. Calibrated brightfield-based imaging for measuring intracellular protein concentration. Cytometry Part A 2018;93A:297–304. (this issue).
33. Pelts M, Pandya SM, Oh CJ, Model MA. Thickness profiling of formaldehyde-fixed cells by transmission-through-dye microscopy. BioTechniques 2011;50:389–396.
34. Lababidi SL, Pelts M, Moitra M, Leff LG, Model MA. Measurement of bacterial volume by transmission-through-dye imaging. J Microbiol Methods 2011;87:375–377.
35. Model MA, Davis MA. Observation of living organisms in environmental samples by transmission-through-dye microscopy. Microsc Today 2016;24:46–50.
36. Schonbrun E, Di Caprio G, Schaak D. Dye exclusion microfluidic microscopy. Opt Express 2013;21:8793–8798.
37. Schonbrun E, Malka R, Di Caprio G, Schaak D, Higgins JM. Quantitative absorption cytometry for measuring red blood cell hemoglobin mass and volume. Cytometry Part A 2014;85A:332–338.
38. Schonbrun E, Di Caprio G. Differentiating neutrophils using the optical coulter counter. J Biomed Opt 2015;20:111205.
39. Gray ML, Hoffman RA, Hansen WP. A new method for cell volume measurement based on volume exclusion of a fluorescent dye. Cytometry 1983;3:428–434.
40. Steen HB, Stokke T. Dye exclusion artifact in flow cytometers. Cytometry 2002;47: 200–205.
41. Becker PL, Fay FS. Cell volume measurement using the digital imaging fluorescence microscope (DIFM). Biophys J 1986;49:465a.
42. Bottier C, Gabella C, Vianay B, Buscemi L, Sbalzarini IF, Meister JJ, Verkhovsky AB. Dynamic measurement of the height and volume of migrating cells by a novel fluorescence microscopy technique. Lab Chip 2011;11:3855–3863.
43. Model MA, Reese JL, Fraizer GC. Measurement of wheat germ agglutinin binding with a fluorescence microscope. Cytometry Part A 2009;75A:874–881.
44. Gabella C, Bertseva E, Bottier C, Piacentini N, Bornert A, Jeney S, Forró L, Sbalzarini IF, Meister JJ, Verkhovsky AB. Contact angle at the leading edge controls cell protrusion rate. Curr Biol 2014;24:1126–1132.
45. Zlotek-Zlotkiewicz E, Monnier S, Cappello G, Le Berre M, Piel M. Optical volume and mass measurements show that mammalian cells swell during mitosis. J Cell Biol 2015;211:765–774.
46. Jin B-J, Verkman AS. Microfluidic platform for rapid measurement of transepithelial water transport. Lab Chip 2017;17:887–895.
47. Davis CE, Rychak JJ, Hosticka B, Davis SC, John JE3, Tucker AL, Norris PM, Moorman JR. A novel method for measuring dynamic changes in cell volume. J Appl Physiol 2004;96:1886–1893.

48. Crowe WE, Wills NK. A simple method for monitoring changes in cell height using fluorescent microbeads and an Ussing-type chamber for the inverted microscope. Pflugers Arch 1991;419:349–357.
49. Srinivas SP, Bonanno JA, Larivière E, Jans D, Van Driessche W. Measurement of rapid changes in cell volume by forward light scattering. Pflugers Arch 2003;447: 97–108.
50. Mege JL, Capo C, Benoliel AM, Foa C, Bongrand P. Study of cell deformability by a simple method. J Immunol Methods 1985;82:3–15.
51. Kao HP, Verkman AS. Tracking of single fluorescent particles in three dimensions: Use of cylindrical optics to encode particle position. Biophys J 1994;67:1291–1300.
52. Roy G, Sauvé R. Effect of anisotonic media on volume, ion and amino-acid content and membrane potential of kidney cells (MDCK) in culture. J Membr Biol 1987;100: 83–96.
53. Kawahara K, Onodera M, Fukuda Y. A simple method for continuous measurement of cell height during a volume change in a single A6 cell. Jpn J Physiol 1994;44: 411–419.
54. Korchev YE, Gorelik J, Lab MJ, Sviderskaya EV, Johnston CL, Coombes CR, Vodyanoy I, Edwards CR. Cell volume measurement using scanning ion conductance microscopy. Biophys J 2000;78:451–457.
55. Maric K, Wiesner B, Lorenz D, Klussmann E, Betz T, Rosenthal W. Cell volume kinetics of adherent epithelial cells measured by laser scanning reflection microscopy: determination of water permeability changes of renal principal cells. Biophys J 2001; 80:1783–1790.
56. Su X, Pang T, Wakabayashi S, Shigekawa M. Evidence for involvement of the putative first extracellular loop in differential volume sensitivity of the Na^+/H^+ exchangers NHE1 and NHE2. Biochemistry 2003;42:1086–1094.
57. Boudreault F, Grygorczyk R. Evaluation of rapid volume changes of substrate-adherent cells by conventional microscopy 3D imaging. J Microsc 2004; 215:302–312.
58. McGrath JJ. A microscope diffusion chamber for the determination of the equilibrium and non-equilibrium osmotic response of individual cells. J Microsc 1985;139: 249–263.
59. Shiba Y, Kanno Y. Survival of BSC-1 cells through the maintenance of cell volume brought about by epidermal growth factor depends on attachment to the substratum. Cell Mol Life Sci 1990;46:492–495.
60. Wang L, Chen L, Zhu L, Rawle M, Nie S, Zhang J, Ping Z, Kangrong C, Jacob TJ. Regulatory volume decrease is actively modulated during the cell cycle. J Cell Physiol 2002;193:110–119.
61. Espelt MV, Mut PN, Amodeo G, Krumschnabel G, Schwarzbaum PJ. Volumetric and ionic responses of goldfish hepatocytes to anisotonic exposure and energetic limitation. J Exp Biol 2003;206:513–522.
62. Wang J, Zhao G, Zhang P, Wang Z, Zhang Y, Gao D, Zhou P, Cao Y. Measurement of the biophysical properties of porcine adipose-derived stem cells by a microperfusion system. Cryobiology 2014;69:442–450.
63. Kudou M, Shiozaki A, Kosuga T, Ichikawa D, Konishi H, Morimura R, Komatsu S, Ikoma H, Fujiwara H, Okamoto K, et al. Inhibition of regulatory volume decrease enhances the cytocidal effect of hypotonic shock in hepatocellular carcinoma. J Cancer 2016;7:1524–1533.
64. Hill DA, Chiosea S, Jamaluddin S, Roy K, Fischer AH, Boyd DD, Nickerson JA, Imbalzano AN. Inducible changes in cell size and attachment area due to expression of a mutant SWI/SNF chromatin remodeling enzyme. J Cell Sci 2004;117:5847–5854.
65. Shapiro H, Parpart AK. The osmotic properties of rabbit and human leucocytes. J Cell Comp Physiol 1937;10:147–163.
66. Kumar PT, Toffalini F, Witters D, Vermeir S, Rolland F, Hertog ML, Nicolaï BM, Puers R, Geeraerd A, Lammertyn J. Digital microfluidic chip technology for water permeability measurements on single isolated plant protoplasts. Sens Actuat B: Chem 2014;199:479–487.
67. Hosoi K, Min KY, Iwagaki A, Murao H, Hanafusa T, Shimamoto C, Katsu K, Kato M, Fujiwara S, Nakahari T. Delayed shrinkage triggered by the Na+-K+ pump in terbutaline-stimulated rat alveolar type II cells. Exp Physiol 2004;89:373–385.
68. Alexopoulos LG, Erickson GR, Guilak F. A method for quantifying cell size from differential interference contrast images: Validation and application to osmotically stressed chondrocytes. J Microsc 2002;205:125–135.
69. Phillips KG, Baker-Groberg SM, McCarty OJ. Quantitative optical microscopy: Measurement of cellular biophysical features with a standard optical microscope. J Vis Exp 2014;86. doi: 10.3791/50988.
70. Tsao YS, Condon RG, Schaefer EJ, Lindsay DA, Liu Z. Biomass and aggregation analysis of human embryonic kidney 293 suspension cell cultures by particle size measurement. Biotechnol Prog 2000;16:809–814.
71. Groulx N, Boudreault F, Orlov SN, Grygorczyk R. Membrane reserves and hypotonic cell swelling. J Membr Biol 2006;214:43–56.
72. Fels J, Orlov SN, Grygorczyk R. The hydrogel nature of mammalian cytoplasm contributes to osmosensing and extracellular pH sensing. Biophys J 2009;96:4276–4285.
73. Boudreault F, Grygorczyk R. Cell swelling-induced ATP release is tightly dependent on intracellular calcium elevations. J Physiol 2004;561:499–513.
74. Docheva D, Padula D, Popov C, Mutschler W, Clausen-Schaumann H, Schieker M. Researching into the cellular shape, volume and elasticity of mesenchymal stem cells, osteoblasts and osteosarcoma cells by atomic force microscopy. J Cell Mol Med 2008; 12:537–552.
75. Andersen LK, Contera SA, Justesen J, Duch M, Hansen O, Chevallier J, Foss M, Pedersen FS, Besenbacher F. Cell volume increase in murine MC3T3-E1 pre-osteoblasts attaching onto biocompatible tantalum observed by magnetic AC mode atomic force microscopy. Eur Cell Mater 2005;10:61–68.
76. Schneider SW, Pagel P, Rotsch C, Danker T, Oberleithner H, Radmacher M, Schwab A. Volume dynamics in migrating epithelial cells measured with atomic force microscopy. Pflugers Arch 2000;439:297–303.
77. Schneider SW, Yano Y, Sumpio BE, Jena BP, Geibel JP, Gekle M, Oberleithner H. Rapid aldosterone-induced cell volume increase of endothelial cells measured by the atomic force microscope. Cell Biol Int 1997;21:759–768.
78. Hessler JA, Budor A, Putchakayala K, Mecke A, Rieger D, Banaszak Holl MM, Orr BG, Bielinska A, Beals J, Baker J. Jr. Atomic force microscopy study of early morphological changes during apoptosis. Langmuir 2005;21:9280–9286.
79. Goerge T, Niemeyer A, Rogge P, Ossig R, Oberleithner H, Schneider SW. Secretion pores in human endothelial cells during acute hypoxia. J Membr Biol 2002;187: 203–211.
80. Quist AP, Rhee SK, Lin H, Lal R. Physiological role of gap-junctional hemichannels. Extracellular calcium-dependent isosmotic volume regulation. J Cell Biol 2000;148: 1063–1074.
81. Lal R, John SA. Biological applications of atomic force microscopy. Am J Physiol 1994;266:C1–21.
82. Hoh JH, Schoenenberger CA. Surface morphology and mechanical properties of MDCK monolayers by atomic force microscopy. J Cell Sci 1994;107:1105–1114.
83. Happel P, Wehner F, Dietzel ID. Scanning ion conductance microscopy – A tool to investigate electrolyte-nonconductor interfaces. In: Méndez-Vilas A, Díaz J, editors. Modern Research and Educational Topics in Microscopy. Badajoz, Spain: Formatex; 2007. pp 968–975.
84. Seifert J, Rheinlaender J, Novak P, Korchev YE, Schäffer TE. Comparison of atomic force microscopy and scanning ion conductance microscopy for live cell imaging. Langmuir 2015;31:6807–6813.
85. Spring KR, Hope A. Fluid transport and the dimensions of cells and interspaces of living Necturus gallbladder. J Gen Physiol 1979;73:287–305.
86. Phillips KG, Jacques SL, McCarty OJ. Measurement of single cell refractive index, dry mass, volume, and density using a transillumination microscope. Phys Rev Lett 2012;109:118105.
87. Gundlach H. Phase contrast and differential interference contrast instrumentation and applications in cell, developmental, and marine biology. Opt Eng 1993;32: 3223–3228.
88. Persson BE, Spring KR. Gallbladder epithelial cell hydraulic water permeability and volume regulation. J Gen Physiol 1982;79:481–505.
89. Errington RJ, Fricker MD, Wood JL, Hall AC, White NS. Four-dimensional imaging of living chondrocytes in cartilage using confocal microscopy: a pragmatic approach. Am J Physiol 1997;272:C1040–C1051.
90. Zelenina M, Brismar H. Osmotic water permeability measurements using confocal laser scanning microscopy. Eur Biophys J 2000;29:165–171.
91. Bettega D, Calzolari P, Doglia SM, Dulio B, Tallone L, Villa AM. Technical report: Cell thickness measurements by confocal fluorescence microscopy on C3H10T1/2 and V79 cells. Int J Radiat Biol 1998; 74:397–403.
92. Satoh H, Delbridge LM, Blatter LA, Bers DM. Surface:volume relationship in cardiac myocytes studied with confocal microscopy and membrane capacitance measurements: species-dependence and developmental effects. Biophys J 1996;70:1494–1504.
93. Tinel H, Wehner F, Sauer H. Intracellular Ca^{2+} release and Ca^{2+} influx during regulatory volume decrease in IMCD cells. Am J Physiol 1994;267:F130–F138.
94. Rappaz B, Barbul A, Emery Y, Korenstein R, Depeursinge C, Magistretti PJ, Marquet P. Comparative study of human erythrocytes by digital holographic microscopy, confocal microscopy, and impedance volume analyzer. Cytometry Part A 2008;73A: 895–903.
95. Yu RC, Abrams DC, Alaibac M, Chu AC. Morphological and quantitative analyses of normal epidermal Langerhans cells using confocal scanning laser microscopy. Br J Dermatol 1994;131:843–848.
96. Guilak F. Volume and surface area measurement of viable chondrocytes in situ using geometric modelling of serial confocal sections. J Microsc 1994;173:245–256.
97. Droste MS, Biel SS, Terstegen L, Wittern KP, Wenck H, Wepf R. Noninvasive measurement of cell volume changes by negative staining. J Biomed Opt 2005;10:064017.
98. Carlsson K. The influence of specimen refractive index, detector signal integration, and non-uniform scan speed on the imaging properties in confocal microscopy. J Microsc 1991;163:167–178.
99. Sheppard CJR, Török P. Effects of specimen refractive index on confocal imaging. J Microsc 1997;185:366–374.
100. van Elburg HJ, Kuypers LC, Decraemer WF, Dirckx JJ. Improved correction of axial geometrical distortion in index-mismatched fluorescent confocal microscopic images using high-aperture objective lenses. J Microsc 2007;228:45–54.
101. Model MA, Fang J, Yuvaraj P, Chen Y, Zhang Newby BM. 3D deconvolution of spherically aberrated images using commercial software. J Microsc 2011;241: 94–100.
102. Hell S, Reiner G, Cremer C, Stelzer EHK. Aberrations in confocal fluorescence microscopy induced by mismatches in refractive index. J Microsc 1993;169: 391–405.
103. Neuman KC, Abbondanzieri EA, Block SM. Measurement of the effective focal shift in an optical trap. Opt Lett 2005;30:1318–1320.
104. Bush PG, Hall AC. The volume and morphology of chondrocytes within non-degenerate and degenerate human articular cartilage. Osteoarthritis Cartilage 2003; 11:242–251.
105. Cohen AR, Roysam B, Turner JN. Automated tracing and volume measurements of neurons from 3-D confocal fluorescence microscopy data. J Microsc 1994;173: 103–114.

106. Bullard TA, Borg TK, Price RL. The expression and role of protein kinase C in neonatal cardiac myocyte attachment, cell volume, and myofibril formation is dependent on the composition. Microsc Microanal 2005;11:224–234.
107. Briggs GAD, Kolosov OV. Acoustic Microscopy, 2nd ed. New York: Oxford University Press; 2010. 356p.
108. Weiss EC, Wehner F, Lemor RM. Measuring cell volume regulation with time resolved acoustic microscopy. Acoust Imag 2007;28:73–80.
109. Plettenberg S, Weiss EC, Lemor R, Wehner F. Subunits α, β and γ of the epithelial Na^+ channel (ENaC) are functionally related to the hypertonicity-induced cation channel (HICC) in rat hepatocytes. Pflugers Arch 2008;455:1089–1095.
110. Bondarava M, Li T, Endl E, Wehner F. αENaC is a functional element of the hypertonicity-induced cation channel in HepG2 cells and it mediates proliferation. Pflugers Arch 2009;458:675–687.
111. Hegner S, Bereiter-Hahn J. Volume determination of adhering cells in culture by means of acoustic interferometry. In: Bernd A, Bereiter-Hahn J, Hevert F, Holzmann H, editors. Cell and Tissue Culture Models in Dermatological Research. Berlin, Heidelberg: Springer; 1993. pp 58–66.
112. Popescu G. Quantitative Phase Imaging of Cells and Tissues. New York: McGraw-Hill; 2011. 385 p.
113. Kim T, Zhou R, Goddard LL, Popescu G. Breakthroughs in photonics 2013: Quantitative phase imaging: Metrology meets biology. IEEE Photonics J 2014;6:1–9.
114. Marquet P, Depeursinge C, Magistretti PJ. Exploring neural cell dynamics with digital holographic microscopy. Annu Rev Biomed Eng 2013;15:407–431.
115. Theisen A, Johann C, Deacon MP, Harding SE. Refractive Increment Data-Book for Polymer and Biomolecular Scientists. Nottingham: Nottingham University Press; 2000. 64p.
116. Rappaz B, Cano E, Colomb T, Kühn J, Depeursinge C, Simanis V, Magistretti PJ, Marquet P. Noninvasive characterization of the fission yeast cell cycle by monitoring dry mass with digital holographic microscopy. J Biomed Opt 2009;14:034049.
117. Curl CL, Bellair CJ, Harris T, Allman BE, Harris PJ, Stewart AG, Roberts A, Nugent KA, Delbridge LM. Refractive index measurement in viable cells using quantitative phase-amplitude microscopy and confocal microscopy. Cytometry Part A 2005; 65A:88–92.
118. Rappaz B, Marquet P, Cuche E, Emery Y, Depeursinge C, Magistretti P. Measurement of the integral refractive index and dynamic cell morphometry of living cells with digital holographic microscopy. Opt Express 2005;13:9361–9373.
119. Rappaz B, Charrière F, Depeursinge C, Magistretti PJ, Marquet P. Simultaneous cell morphometry and refractive index measurement with dual-wavelength digital holographic microscopy and dye-enhanced dispersion of perfusion medium. Opt Lett 2008;33:744–746.
120. Boss D, Kühn J, Jourdain P, Depeursinge C, Magistretti PJ, Marquet P. Measurement of absolute cell volume, osmotic membrane water permeability, and refractive index of transmembrane water and solute flux by digital holographic microscopy. J Biomed Opt 2013;18:036007.
121. Farinas J, Verkman AS. Cell volume and plasma membrane osmotic water permeability in epithelial cell layers measured by interferometry. Biophys J 1996;71: 3511–3522.
122. Farinas J, Kneen M, Moore M, Verkman AS. Plasma membrane water permeability of cultured cells and epithelia measured by light microscopy with spatial filtering. J Gen Physiol 1997;110:283–296.
123. Charrière F, Pavillon N, Colomb T, Depeursinge C, Heger TJ, Mitchell EA, Marquet P, Rappaz B. Living specimen tomography by digital holographic microscopy: morphometry of testate amoeba. Opt Express 2006;14:7005–7013.
124. Sung Y, Choi W, Fang-Yen C, Badizadegan K, Dasari RR, Feld MS. Optical diffraction tomography for high resolution live cell imaging. Opt Express 2009;17: 266–277.
125. Kim Y, Shim H, Kim K, Park H, Heo JH, Yoon J, Choi C, Jang S, Park Y. Common-path diffraction optical tomography for investigation of three-dimensional structures and dynamics of biological cells. Opt Express 2014;22:10398–10407.
126. Kim T, Zhou R, Mir M, Babacan SD, Carney PS, Goddard LL, Popescu G. White-light diffraction tomography of unlabeled live cells. Nat Photonics 2014;8:256–263.
127. Niclis JC, Murphy SV, Parkinson DY, Zedan A, Sathananthan AH, Cram DS, Heraud P. Three-dimensional imaging of human stem cells using soft X-ray tomography. J R Soc Interface 2015;12:20150252.
128. Hanssen E, Knoechel C, Dearnley M, Dixon MW, Le Gros M, Larabell C, Tilley L. Soft X-ray microscopy analysis of cell volume and hemoglobin content in erythrocytes infected with asexual and sexual stages of Plasmodium falciparum. J Struct Biol 2012;177:224–232.
129. Reuss L. Changes in cell volume measured with an electrophysiologic technique. Proc Natl Acad Sci USA 1985;82:6014–6018.
130. Alvarez-Leefmans FJ, Gamiño SM, Reuss L. Cell volume changes upon sodium pump inhibition in Helix aspersa neurones. J Physiol 1992;458:603–619.
131. Adorante JS. Regulatory volume decrease in frog retinal pigment epithelium. Am J Physiol 1995;268:C89–C100.
132. Dierkes PW, Coulon P, Neumann S, Schlue WR. Potentiometric measurement of cell volume changes and intracellular ion concentrations under voltage-clamp conditions in invertebrate nerve cells. Anal Bioanal Chem 2002;373:762–766.
133. Tauc M, Le Maout S, Poujeol P. Fluorescent video-microscopy study of regulatory volume decrease in primary culture of rabbit proximal convoluted tubule. Biochim Biophys Acta 1990;1052:278–284.
134. Muallem S, Zhang BX, Loessberg PA, Star RA. Simultaneous recording of cell volume changes and intracellular pH or Ca^{2+} concentration in single osteosarcoma cells UMR-106–01. J Biol Chem 1992;267:17658–17664.
135. Model MA. Intensity calibration and shading correction for fluorescence microscopes. Curr Protoc Cytom 2014;68:10.14.1–10.14.10.
136. Crowe WE, Altamirano J, Huerto L, Alvarez-Leefmans FJ. Volume changes in single N1E-115 neuroblastoma cells measured with a fluorescent probe. Neuroscience 1995;69:283–296.
137. Farinas J, Simanek V, Verkman AS. Cell volume measured by total internal reflection microfluorimetry: application to water and solute transport in cells transfected with water channel homologs. Biophys J 1995;68:1613–1620.
138. Chen Z, Zhang Z, Gu Y, Bai C. Impaired migration and cell volume regulation in aquaporin 5-deficient SPC-A1 cells. Respir Physiol Neurobiol 2011;176:110–117.
139. Mola MG, Sparaneo A, Gargano CD, Spray DC, Svelto M, Frigeri A, Scemes E, Nicchia GP. The speed of swelling kinetics modulates cell volume regulation and calcium signaling in astrocytes: A different point of view on the role of aquaporins. Glia 2016;64:139–154.
140. Kim YK, Illsley NP, Verkman AS. Rapid fluorescence assay of glucose and neutral solute transport using an entrapped volume indicator. Anal Biochem 1988;172: 403–409.
141. Wehner F, Sauer H, Kinne RK. Hypertonic stress increases the Na^+ conductance of rat hepatocytes in primary culture. J Gen Physiol 1995;105:507–535.
142. Wehner F, Tinel H. Osmolyte and Na^+ transport balances of rat hepatocytes as a function of hypertonic stress. Pflugers Arch 2000;441:12–24.
143. Hamann S, Kiilgaard JF, Litman T, Alvarez-Leefmans FJ, Winther BR, Zeuthen T. Measurement of cell volume changes by fluorescence self-quenching. J Fluorescence 2002;12:139–145.
144. Pafundo DE, Alvarez CL, Krumschnabel G, Schwarzbaum PJ. A volume regulatory response can be triggered by nucleosides in human erythrocytes, a perfect osmometer no longer. J Biol Chem 2010;285:6134–6144.
145. Precourt DM. Assessment of calcein dye method to observe cell volume regulation. Forensic Science Theses (Master of Science), Paper 10. 2016.
146. Solenov E, Watanabe H, Manley GT, Verkman AS. Sevenfold-reduced osmotic water permeability in primary astrocyte cultures from AQP-4-deficient mice, measured by a fluorescence quenching method. Am J Physiol Cell Physiol 2004;286: C426–C432.
147. Davidson AF, Higgins AZ. Detection of volume changes in calcein-stained cells using confocal microscopy. J Fluoresc 2013;23:393–398.
148. Benfenati V, Caprini M, Dovizio M, Mylonakou MN, Ferroni S, Ottersen OP, Amiry-Moghaddam M. An aquaporin-4/transient receptor potential vanilloid 4 (AQP4/TRPV4) complex is essential for cell-volume control in astrocytes. Proc Natl Acad Sci USA 2011;108:2563–2568.
149. Capó-Aponte JE, Iserovich P, Reinach PS. Characterization of regulatory volume behavior by fluorescence quenching in human corneal epithelial cells. J Membr Biol 2005;207:11–22.
150. Voss FK, Ullrich F, Münch J, Lazarow K, Lutter D, Mah N, Andrade-Navarro MA, von Kries JP, Stauber T, Jentsch TJ. Identification of LRRC8 heteromers as an essential component of the volume-regulated anion channel VRAC. Science 2014;344: 634–638.
151. Jin BJ, Esteva-Font C, Verkman AS. Droplet-based microfluidic platform for measurement of rapid erythrocyte water transport. Lab Chip 2015;15:3380–3390.
152. Srinivas SP, Bonanno JA. Measurement of changes in cell volume based on fluorescence quenching. Am J Physiol 1997;272:C1405–C1414.
153. Jentsch TJ. VRACs and other ion channels and transporters in the regulation of cell volume and beyond. Nat Rev Mol Cell Biol 2016;17:293–307.
154. Fraser JA, Huang CL. Quantitative techniques for steady-state calculation and dynamic integrated modelling of membrane potential and intracellular ion concentrations. Prog Biophys Mol Biol 2007;94:336–372.
155. Baumgart F, Rossi A, Verkman AS. Light inactivation of water transport and protein-protein interactions of aquaporin-Killer Red chimeras. J Gen Physiol 2012; 139:83–91.
156. Esteva-Font C, Phuan PW, Anderson MO, Verkman AS. A small molecule screen identifies selective inhibitors of urea transporter UT-A. Chem Biol 2013;20: 1235–1244.
157. Bregestovski P, Waseem T, Mukhtarov M. Genetically encoded optical sensors for monitoring of intracellular chloride and chloride-selective channel activity. Front Mol Neurosci 2009;2:15.
158. Arosio D, Ratto GM. Twenty years of fluorescence imaging of intracellular chloride. Front Cell Neurosci 2014;8:258.
159. Arosio D, Ricci F, Marchetti L, Gualdani R, Albertazzi L, Beltram F. Simultaneous intracellular chloride and pH measurements using a GFP-based sensor. Nat Methods 2010;7:516–518.
160. Kinnunen M, Karmenyan A. Overview of single-cell elastic light scattering techniques. J Biomed Opt 2015;20:051040.
161. Drezek R, Dunn A, Richards-Kortum R. Light scattering from cells: finite-difference time-domain simulations and goniometric measurements. Appl Opt 1999;38:3651–3661.
162. Mulvey CS, Curtis AL, Singh SK, Bigio IJ. Elastic scattering spectroscopy as a diagnostic tool for apoptosis in cell cultures. IEEE J Sel Topics Quantum Electron 2007; 13:1663–1670.
163. Mulvey CS, Zhang K, Bobby Liu WH, Waxman DJ, Bigio IJ. Wavelength-dependent backscattering measurements for quantitative monitoring of apoptosis, part 2: early spectral changes during apoptosis are linked to apoptotic volume decrease. J Biomed Opt 2011;16:117002.
164. Tzur A, Moore JK, Jorgensen P, Shapiro HM, Kirschner MW. Optimizing optical flow cytometry for cell volume-based sorting and analysis. PLoS One 2011;6: e16053.

165. Salzman CS. Light scatter: detection and usage. Curr Protoc Cytom 1999;9: 1.13.1–1.13.8.
166. Shapiro HM. Practical Flow Cytometry, 4th ed. Hoboken, NJ: Wiley. 2003. 736p.
167. Mohandas N, Kim YR, Tycko DH, Orlik J, Wyatt J, Groner W. Accurate and independent measurement of volume and hemoglobin concentration of individual red cells by laser light scattering. Blood 1986;68:506–513.
168. Zwicker JI. Impedance-based flow cytometry for the measurement of microparticles. Semin Thromb Hemost 2010;36:819–823.
169. Anderson EC, Petersen DF, Tobey RA. Density invariance of cultured Chinese hamster cells with stage of the mitotic cycle. Biophys J 1970;10:630–645.
170. Loken MR, Kubitschek HE. Constancy of cell buoyant density for cultured murine cells. J Cell Physiol 1984;118:22–26.
171. Yeung CH, Anapolski M, Cooper TG. Measurement of volume changes in mouse spermatozoa using an electronic sizing analyzer and a flow cytometer: validation and application to an infertile mouse model. J Androl 2002;23:522–528.
172. Downey GP, Grinstein S, Sue-A-Quan A, Czaban B, Chan CK. Volume regulation in leukocytes: Requirement for an intact cytoskeleton. J Cell Physiol 1995;163: 96–104.
173. Keller HU, Fedier A, Rohner R. Relationship between light scattering in flow cytometry and changes in shape, volume, and actin polymerization in human polymorphonuclear leukocytes. J Leukoc Biol 1995;58:519–525.
174. McGann LE, Walterson ML, Hogg LM. Light scattering and cell volumes in osmotically stressed and frozen-thawed cells. Cytometry 1988;9:33–38.
175. Sloot PM, Hoekstra AG, Figdor CG. Osmotic response of lymphocytes measured by means of forward light scattering: Theoretical considerations. Cytometry 1988;9: 636–641.
176. Pozarowski P, Grabarek J, Darzynkiewicz Z. Flow cytometry of apoptosis. Curr Protoc Cytom 2003;25:7.19.1–7–19.33.
177. Ormerod MG, Paul F, Cheetham M, Sun XM. Discrimination of apoptotic thymocytes by forward light scatter. Cytometry 1995;21:300–304.
178. Zamai L, Falcieri E, Zauli G, Cataldi A, Vitale M. Optimal detection of apoptosis by flow cytometry depends on cell morphology. Cytometry 1993;14:891–897.
179. Mlekoday HJ, Moore R, Levitt DG. Osmotic water permeability of the human red cell. Dependence on direction of water flow and cell volume. J Gen Physiol 1983;81: 213–220.
180. Yang B, Kim JK, Verkman AS. Comparative efficacy of HgCl2 with candidate aquaporin-1 inhibitors DMSO, gold, TEA+ and acetazolamide. FEBS Lett 2006; 580:6679–6684.
181. Parpart AK. The permeability of the mammalian erythrocyte to deuterium oxide (heavy water). J Cell Physiol 1935;7:153–162.
182. Lucké B, Parpart AK. Osmotic properties and permeability of cancer cells. I. Relative permeability of Ehrlich mouse ascites tumor cells and of mouse erythrocytes to polyhydric alcohols and to sodium chloride. Cancer Res 1954;14:75–80.
183. Hempling HG. Permeability of the Ehrlich ascites tumor cell to water. J Gen Physiol 1960;44:365–379.
184. Sidel VW, Solomon AK. Entrance of water into human red cells under an osmotic pressure gradient. J Gen Physiol 1957;41:243–257.
185. Knauf PA, Fuhrmann GF, Rothstein S, Rothstein A. The relationship between anion exchange and net anion flow across the human red blood cell membrane. J Gen Physiol 1977;69:363–386.
186. Dho S, Chou S, Chang XB, Rommens JM, Foskett JK. Right-angle light scattering to assay basal and regulated plasma membrane Cl^- conductances. Am J Physiol 1992;263:C530–C534.
187. Brunsting A, Mullaney PF. Differential light scattering from spherical mammalian cells. Biophys J 1974;14:439–453.
188. Fischbarg J, Kuangt K, Hirsch J, Lecuona S, Rogozinski L, Silverstein SC, Loike J. Evidence that the glucose transporter serves as a water channel in J774 macrophages. Proc Natl Acad Sci USA 1989;86:8397–8401.
189. Fischbarg J, Li J, Kuang K, Echevarría M, Iserovich P. Determination of volume and water permeability of plated cells from measurements of light scattering. Am J Physiol 1993;265:C1412–C1423.
190. Echevarria M, Verkman AS. Optical measurement of osmotic water transport in cultured cells. Role of glucose transporters. J Gen Physiol 1992;99:573–589.
191. McManus M, Fischbarg J, Sun A, Hebert S, Strange K. Laser light-scattering system for studying cell volume regulation and membrane transport processes. Am J Physiol 1993;265:C562–C570.
192. Kuang K, Yiming M, Zhu Z, Iserovich P, Diecke FP, Fischbarg J. Lack of threshold for anisotonic cell volume regulation. J Membr Biol 2006;211:27–33.
193. Spitzer MH, Nolan GP. Mass cytometry: Single cells, cany features. Cell 2016;165: 780–791.
194. Stern AD, Rahman AH, Birtwistle MR. Cell size assays for mass cytometry. Cytometry Part A 2017;91A:14–24.
195. Savitz D, Sidel VW, Solomon AK. Osmotic properties of human red cells. J Gen Physiol 1964;48:79–94.
196. Bratbak G, Dundas I. Bacterial dry matter content and biomass estimations. Appl Environ Microbiol 1984;48:755–757.
197. Kubitschek HE, Friske JA. Determination of bacterial cell volume with the Coulter Counter. J Bacteriol 1986;168:1466–1467.
198. Kletzien RF, Pariza MW, Becker JE, Potter VR. A method using 3-O-methyl-D-glucose and phloretin for the determination of intracellular water space of cells in monolayer culture. Anal Biochem 1975;68:537–544.
199. O'Donnell ME, Brandt JD, Curry FR. Na-K-Cl cotransport regulates intracellular volume and monolayer permeability of trabecular meshwork cells. Am J Physiol 1995;268:C1067–C1074.
200. Weiss L. The effects of trypsin on the size, viability and dry mass of sarcoma 37 cells. Exp Cell Res 1958;14:80–83.
201. Mallucci L, Wells V, Young MR. Effect of trypsin on cell volume and mass. Nat New Biol 1972;239:53–55.
202. Montesinos E, Esteve I, Guerrero R. Comparison between direct methods for determination of microbial cell volume: Electron microscopy and electronic particle sizing. Appl Environ Microbiol 1983;45:1651–1658.
203. Choi JW, Stoecker DK. Effects of fixation on cell volume of marine planktonic protozoa. Appl Environ Microbiol 1989;55:1761–1765.
204. Crawford CNC, Barer R. The action of formaldehyde on living cells as studied by phase-contrast microscopy. J Cell Sci 1951;3:403–452.
205. Fox CH, Johnson FB, Whiting J, Roller PP. Formaldehyde fixation. J Histochem Cytochem 1985;33:845–853.
206. Bacallao R, Sohrab S, Phillips C. Guiding principles of specimen preservation for confocal fluorescence microscopy. In: Pawley JB, editor. Handbook of biological confocal microscopy, 3rd ed. New York: Springer; 2006. pp 368–380.